JOURNAL OF THE
HYDRAULICS DIVISION

Purchased by
U.S. Department of Agriculture
for Official Use

Rainfall Excess Model from Soil Water Flow Theory[a]

Roger E. Smith[1] and Don L. Chery, Jr.,[2] Associate Members, ASCE

Introduction

Of all the movement and transformation processes to which water is subjected in the lithospheric part of the hydrologic cycle, infiltration is perhaps second only to evapotranspiration in complexity. In the semiarid plains of the western United States and similar areas, these two may be the only important processes moving soil water, since the ground water is essentially disconnected from the surface except at large alluvial channels. Infiltration governs disposition of rainwater at the soil surface, which affects runoff not only for the immediate storm but, along with evapotranspiration, affects the soil water content and thus the infiltration rate at the start of the next rainfall.

Perhaps because of its complexity, hydrologists have tended either to ignore infiltration or to characterize it with gross simplifications. Surface water hydrologists have presumed soil infiltration to be a topic for ground-water hydrologists, and ground-water hydrologists have assumed that surface water hydrologists will provide "input" data for their work. Hydrologic research has produced countless theories and models that assume a value of "rainfall excess" is somehow known or can be calculated.

Meanwhile, research in unsaturated porous media flow, utilizing the growing capabilities of the digital computer, is producing multidimensional solutions to

Note.—Discussion open until February 1, 1974. To extend the closing date one month, a written request must be filed with the Editor of Technical Publications, ASCE. This paper is part of the copyrighted Journal of the Hydraulics Division, Proceedings of the American Society of Civil Engineers, Vol. 99, No. HY9, September, 1973. Manuscript was submitted for review for possible publication on January 18, 1973.

[a]Presented at the August 16-18, 1972, ASCE Hydraulics Division Specialty Conference, held at Ithaca College, Ithaca, N.Y.

[1]Research Hydr. Engr., Southwest Watershed Research Center, Agric. Research Service, USDA, Tucson, Ariz.

[2]Research Hydr. Engr., Southwest Watershed Research Center, Agric. Research Service, USDA, Tucson, Ariz.

complex systems of partial differential equations that represent realistic approximations to the soil system response to rainfall input (1).

The soil moisture storage model presented herein is a parametric mimic of a numerical solution of a partial differential equation for unsaturated flow from infiltration. This model is incorporated in a comprehensive model of small plot response, and is used to predict several runoff events. Each prediction is compared with that of a comparable empirical model.

Underlying Soil Moisture Flow Theory

The differential equations describing unsaturated flow in porous media are simply combinations of Darcy's Law and the law of continuity. Two fluid phases

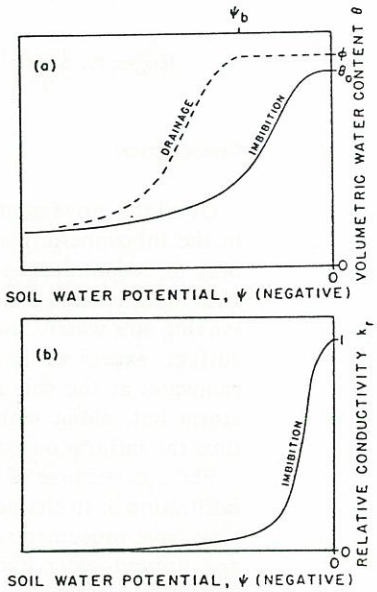

FIG. 1.—Example Soil Water Potential-Volumetric Saturation-Relative Conductivity Relationships

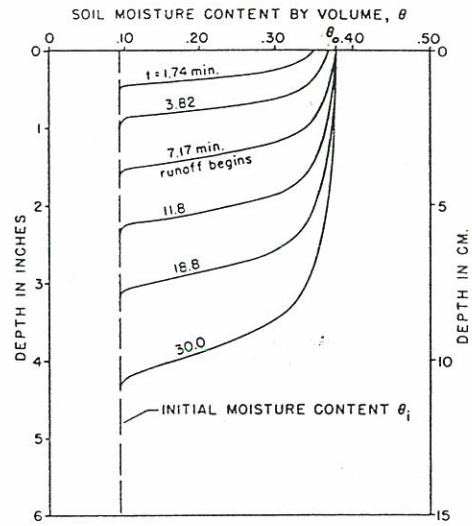

FIG. 2.—Sample Results of Numerical Solution of Eq. 1 for Advance of Wetting Front in Sandy Loam Soil

are involved—as water enters a particular volume of soil, air must flow out. Description of both phases involves two simultaneous partial differential equations. Where air can move freely, or where the water table is at considerable depth, air is assumed to move under negligible pressure gradients and a single partial differential equation for water flow is

$$\phi \frac{\partial \theta}{\partial t} = K \frac{\partial}{\partial z}\left(k_r \frac{\partial \psi}{\partial z}\right) - K \frac{\partial k_r}{\partial z} \quad (1)$$

in which ψ = soil water potential, L; z = depth from the soil surface, L; θ = moisture content by volume; k_r = relative permeability or conductivity; K = saturated conductivity, L/T; t = time, T; and ϕ = porosity. The keys

to the solution of Eq. 7 are the interrelation of k_r and ψ, and of θ and ψ, known as the relative conductivity-tension curve and the moisture-tension curve, respectively (see Fig. 1). It is inappropriate to attempt to examine soil water

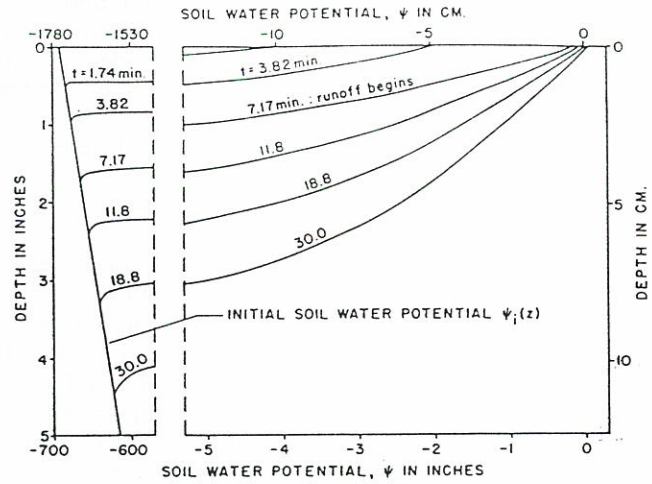

FIG. 3.—Sample Results of Numerical Solution of Eq. 1 for Development of Soil Water Potential Profile in Sandy Loam Soil

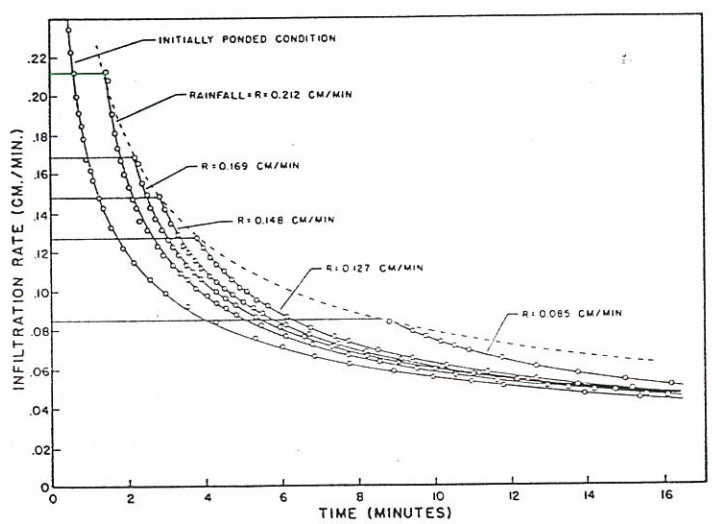

FIG. 4.—Typical Family of Infiltration Decay Curves Produced by Solution of Eq. 1 for Infiltrating Soil Column

flow theory in detail herein. Gardner (2) gives a good outline of the development of this equation in soil physics. McWhorter (6) has presented an excellent treatise on infiltration where air flow is not neglected.

With Eq. 1, soil water movement from rainfall or ponding is treated as a boundary value problem. Fig. 2 shows a typical solution in (θ, z), and Fig. 3 shows a solution in (ψ, z) for selected values of t for a sample soil. With appropriate numerical methods, and a sufficiently precise array of grid sizes, one also may obtain solutions from Eq. 1 describing infiltration rates for a variety of initial and upper boundary conditions (8). These theoretical solutions for infiltration patterns under a variety of conditions will be presented as a dimensionless system whose principal dependent variable is cumulative infiltrated soil water.

Theoretically Based Infiltration Model

Parameterization of Numerical Solution Results.—Fig. 4 is a graphical presentation of infiltration from the numerical solution of Eq. 1. The first curve represents infiltration decay from initial sudden ponding at the soil surface. The remaining curves are identified by the various uniform rainfall rates, R, maintained at the surface. Infiltration proceeds at the rainfall rate until a time, $t_p = t_p R$, at which the soil potential, ψ, at the surface reaches 0, after which the infiltration rate decreases with time as an exhaustion phenomenon. The loci of points $t_p R$ form a curve that has been termed the "infiltration envelope" (7).

The curves of Fig. 4 may each be closely described (7) by an equation of the form

$$f = f_\infty + A(t - t_o)^{-\alpha} \quad \text{for} \quad t > t_p \qquad (2)$$

in which $f_\infty = K$ by theory; and A, t_o, and α = parameters. Term $t_o = 0$ for infiltration from a ponded upper boundary condition, in which case Eq. 2 is very similar to the Kostiakov infiltration formula (5). This family of curves may be unified, using a dimensionless expression, by defining $f_* = f/f_\infty$, $r_* = R/f_\infty$, and $t_* = t/T_o$; the star indicates a dimensionless quantity. Normalizing time T_o is defined by

$$\int_0^{T_o} A s^{-\alpha}\, ds = f_\infty T_o \qquad (3)$$

in which s = a variable of integration. Eq. 3 may be solved for T_o, and these nondimensionalizing definitions allow Eq. 2 to be expressed as

$$f_* - 1 = (1 - \alpha)(t_* - t_{o*})^{-\alpha} \qquad (4)$$

It is interesting to note briefly that Eq. 4 implies that a simplified model exists for representing the infiltration rates predicted by soil water flow theory, as in Eq. 1. The simplified model relates infiltration rate to a nonlinear function of soil water storage. Consider, e.g., the case of initially ponded infiltration, in which $t_o = 0$. Let $f_*' = f_* - 1$ and let Q_*' represent dimensionless accumulated soil water in excess of $(f_{\infty *} t_*)$ (note that $f_{\infty *} = 1$). Then the relation

$$f_*' = \frac{dQ_*'}{dt^*} = \frac{C}{(Q_*')^n} \qquad (5)$$

may be integrated to yield Eq. 4 under the conditions that

$$C = 1 - \alpha \quad \text{and} \quad n = \frac{\alpha}{1 - \alpha} \qquad (6)$$

The relation in Eq. 5 may be extended to rainfall infiltration (see Appendix I), in which Q_*' is replaced by $(Q_*' - Q_{o*})$, in which Q_{o*} is analogous to t_{o*}; C and n are related to α as shown previously, and Eq. 5 may be written as a function of dimensionless infiltrated volume:

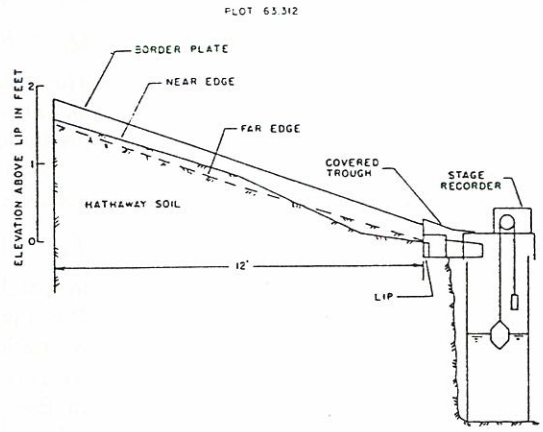

FIG. 5.—Profile Sketch of 6 ft × 12 ft Runoff Plot Used to Study Accuracy of Theoretical Infiltration Model

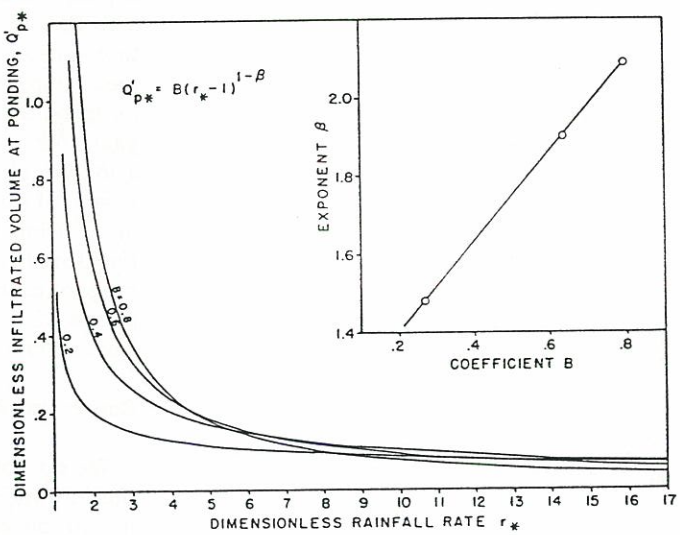

FIG. 6.—Dimensionless Infiltration Envelope Curves Describing Time of Runoff as Function of Rainfall Rate and Soil Related Parameter B

$$f'_* = (1 - \alpha)(Q'_* - Q_{o*})^{-\alpha/(1-\alpha)} \quad (7)$$

The infiltration envelope also has an important relationship with infiltrated volume. Define $Q'_{p*} = t_{p*}(r_* - 1)$, which is the infiltrated volume at ponding in excess of $f_{\infty*} t_{p*}$. Experimental results with different patterns of rainfall [Smith (7)] indicate that Q'_{p*} may be used to predict ponding time t_{p*} for any precipitation pattern, since no matter what the previous rainfall rates, ponding will occur whenever $Q'_* \geq Q'_{p*}$ for the current rainfall rate, r_*. From solution results of Eq. 1, Q'_{p*} is related to rainfall rate by

$$Q'_{p*} = B(r_* - 1)^{1-\beta} \quad (8)$$

This relationship is shown in Fig. 5. Parameters B and β are, from limited amounts of testing, apparently related as in the inset of Fig. 6. This allows prediction of one by the other.

Finally, normalizing time T_o appears from experiments to be predicted accurately as a function of initial saturation deficit, such that

$$T_o = D(\theta_o - \theta_i) \quad (9)$$

in which θ_o is θ at $\psi = 0$ [Fig. 1(a)] and θ_i is initial water content. In effect, D is a measure of the sensitivity of infiltration to changes in initial soil moisture. Numerical solutions indicate such sensitivity increases markedly from sands with low sensitivity ($D \sim 50$ min) to clays ($D \sim 5{,}000$ min). The simple relationships in Eqs. 7, 8, and 9 constitute the numerical soil-equivalent model, hereafter referred to as SEQM.

Determining Model Parameters.—The four basic parameters of SEQM presented previously are f_∞, α, B, and D. Value Q_o may be computed from Eq. 7 after determining Q'_{p*} from Eq. 8 using $Q_* = Q'_{p*}$ at $f_* = r_*$ (the point when runoff begins). Parameters f_∞ and D can be determined experimentally, leaving B and α to be estimated. A somewhat less explicitly objective procedure allows one to estimate all four parameters from one infiltrometer experiment, as used in the example to follow. Value f_∞ is estimated as the apparent long-time asymptote by using an arithmetic plot of f versus t. Then t_o (Eq. 2) is selected as that value for which $(f - f_\infty)$ versus $(t - t_o)$ is most closely a straight line on a log-log plot. Value α and A (Eq. 2) are then the slope and intercept ($t - t_o = 1$) of this line. From Eq. 3, T_o may be computed, which allows computation of D using Eq. 9. Value B can be estimated from Eq. 8 using Q'_{p*} and r_* (measured) and the relation for B and β in Fig. 5. Fortunately, the apparent range of each of these parameters is small, although their effect is often sensitive; values of α from 0.55 to 0.8 have been determined, while B has a range at least from 0.55 to 0.9.

Comparative Application in Predicting Plot Runoff

We do not propose in this paper to attempt an experimental verification of the infiltration model presented in the preceding section. Hydrologic research has produced a wide assortment of infiltration decay formulas, all based on experimental "verification." Experiments have been reported in the literature to indicate the appropriateness of Eq. 1 in describing soil water movement in homogeneous soil (2,6,7,8,9). Other experiments have been reported that

should convince the most optimistic theoretician that natural soil is more often nonhomogeneous than otherwise, and that the neglect of air-phase movement can in many cases be serious (6). The overall object of infiltration prediction in this research is the prediction of rainfall excess on small source watersheds in the semiarid plains of the Southwest, where streamflow results almost exclusively from surface water runoff. Lacking adequate laboratory facilities for soil infiltration study, we are attempting to apply the infiltration model directly to predict runoff from small 6 ft × 12 ft (3 m × 4 m) plots. A soil plot model has been constructed of totally "deterministic" components (considering the SEQM to be effectively deterministic), including kinematic routing of

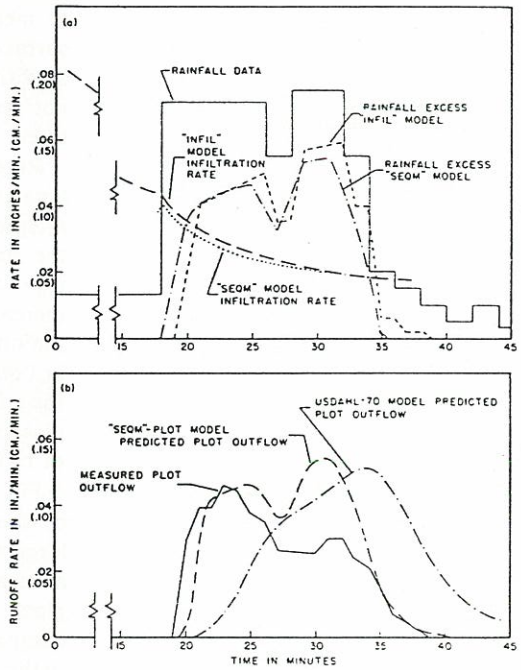

FIG. 7.—Measured and Predicted Rainfall Excess and Plot Runoff for One Event (September 10, 1967) on Experimental Plot

the rainfall excess over the rough surfaces and explicit interaction of surface conditions and infiltration rates.

A type F infiltrometer experiment provided data for deducing the parameters in SEQM. Runoff from several natural storms was then predicted for a different plot having supposedly the same soil type as in the infiltrometer plot. An empirical infiltration model (INFIL subroutine of watershed model USDAHL-70) developed by Holtan (4) has been chosen for comparison with the aforementioned SEQM model. From personal communication with Holtan, the infiltration relation has been modified to $f = \mathrm{GI}\ a\ S_{\alpha}^{G/AWC} + f_c$. This recent modification has not yet appeared in the literature, but is very significant in obtaining the results shown herein. The configuration of the INFIL model used for this evalution has eight

parameters. Infiltration is computed as a function of a variable, S_a, which is described as a representation of available soil pore volume. Seven parameters were obtained by trial and error estimation using three earlier events, assuming no initial wetness, on the same runoff plot. One of these test events is the example in Fig. 7. The initial wetness of the soil is represented by the eighth parameter, termed ASM.

The prediction attempts considered subsequently were made for a gravelly sandy loam with very little vegetative cover. The plot and runoff measurement arrangement is shown in Fig. 5. Although some surface routing occurs on these plots, the hydrograph is relatively insensitive to slope and roughness, which would be important parameters for a larger watershed response. Comparison of mean rainfall excess with plot outflow in Fig. 7 indicates the amount of surface storage at any time. For use in the predictions, measured rainfall was modified slightly at sharp rate changes by specifying that rainfall rates must not be discontinuous. Thus discontinuities were changed to rapidly changing rates.

Results.—Fig. 7(*a*) shows predictions from SEQM and the USDAHL-70 model. One important point is well illustrated by this example—the inadequacy of integrating gages for small-scale runoff prediction. The record indicates that the second high burst of rainfall is higher than the first, yet recorded runoff is lower on the second peak. Since this could occur only if infiltration somehow increased dramatically rather than decayed, one must conclude that the differentiation of the integrating (weighing) rain gage, or the integrating runoff gage, or both, has not accurately assessed the respective rate pattern. Fig. 7(*a*) shows the effect on rainfall excess patterns when rainfall rate discontinuities are disallowed. The SEQM rainfall excess pattern shown has short time periods of rapidly changing rate instead of discontinuities.

Fig. 7(*a*) also demonstrates the comparative prediction of infiltration rates by the soil model and the INFIL model. For rainfall bursts that are relatively large with respect to infiltration capacity, any infiltration model which produces a decay-type curve dividing the rainfall hyetograph at approximately the same place will produce similar rainfall excess. In many cases this applies to the comparisons reported herein. Apparently, a numerical bias in continuity exists in the INFIL model, in that rainfall excess is some 5% greater than the difference between rainfall and infiltration capacity.

Runoff prediction is demonstrated further by the following figures for a series of events on runoff plot for which comparatively accurate runoff and initial soil moisture data were available. The USDAHL-70 model does not adequately model surface routing on these small plots, as demonstrated in Fig. 7(*b*); therefore, only predicted rainfall excess (INFIL subroutine) is shown for the USDAHL-70 model. The writers feel that comparison of predicted plot runoff would perhaps be unfair knowing this bias exists. Because of the small effect of surface routing, the comparison is, in effect, for the infiltration models.

Electrical resistance blocks provide a relative indication of initial soil moisture for these data, and the resistance readings, rainfall, and interpreted soil moisture changes for the period are shown in Fig. 8. For all plot measurements the rainfall and runoff record timing can be assumed accurate only to within ± 2 min to 3 min. Some records are obviously displaced more than that.

The event of July 23, 1971 (Fig. 9) occurred when the soil was relatively

dry (see Fig. 8). Small variable rates of rainfall were measured for about 30 min before runoff began. SEQM under-predicted the amount of runoff from this low-intensity storm, but timing of response was very good. INFIL predicted no runoff.

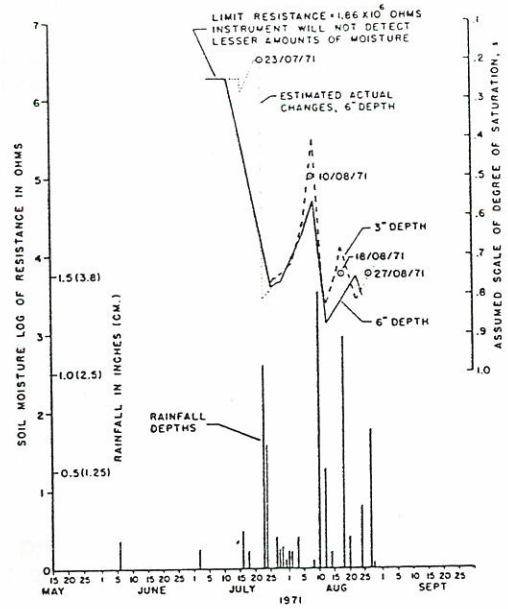

FIG. 8.—Recorded Resistance of Soil Moisture Block in Experimental Plot and Assumed Corresponding Volumetric Soil Water Saturation Interpreted for Initial Conditions in Period of Study

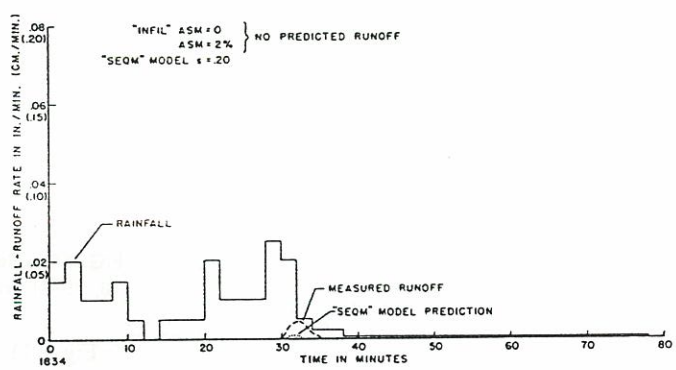

FIG. 9.—Recorded and Predicted Runoff from Low Intensity Rainfall Event (July 23, 1971) Under Relatively Dry Initial Soil Conditions

Fig. 10 shows predicted and measured runoff from a moderately heavy shower. In this example it is reasonable to assume a 1-min or 2-min timing error in

the data. This event also indicates some severe noise incorporated in the runoff data by differentiation of accumulated runoff measurement with a time scale four times more sensitive than records obtained before 1971. The processing of the more damped September 10, 1967 record (Fig. 7) did not result in such noise. The second peak in the second hydrograph is also not supported by any associated rainfall peak, indicating inadequacy in rainfall rate information. On the whole, both the INFIL model and SEQM appear to do comparably well on this event.

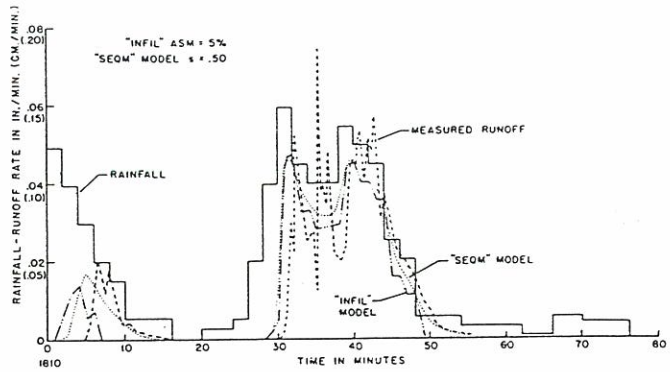

FIG. 10.—Recorded and Predicted Runoff for Multiple Burst Rainfall Event (August 10, 1971) on Moderately Moist Soil

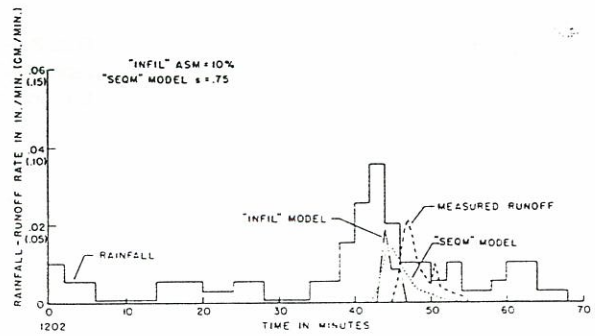

FIG. 11.—Recorded and Predicted Runoff from Low Intensity Complex Rain (August 18, 1971) on Relatively Moist Soil

Figs. 11 and 12 show a relatively small and large runoff event when the experimental plot was initially wet. Again both models predicted plot runoff reasonably well, and again the timing between measured data is doubtful. For the large flow in Fig. 12, there is a discrepancy in the length of runoff time, independent of a time shift between rainfall and runoff. Apparently both predictions are high in runoff volume or at least total time of runoff.

Analysis.—Comparison of the two rainfall excess models show that each predicts a rainfall excess that is generally close to that measured from a 6-ft × 12-ft

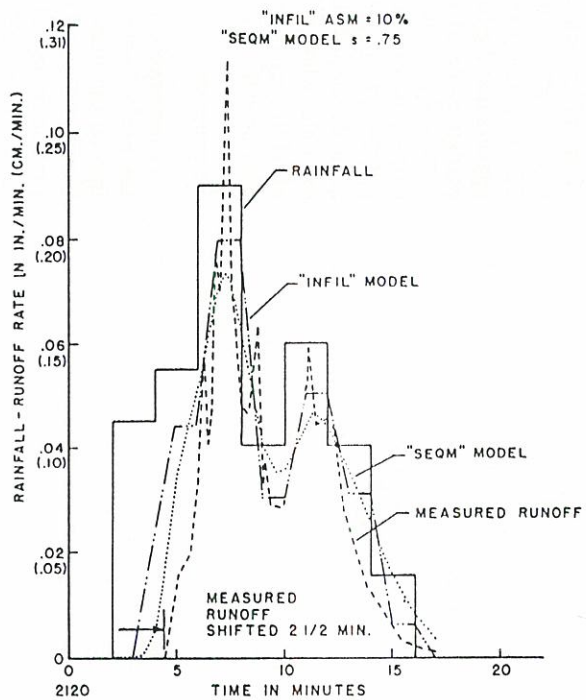

FIG. 12.—Recorded and Predicted Runoff from High Intensity Rainfall (August 27, 1971) on Relatively Moist Soil

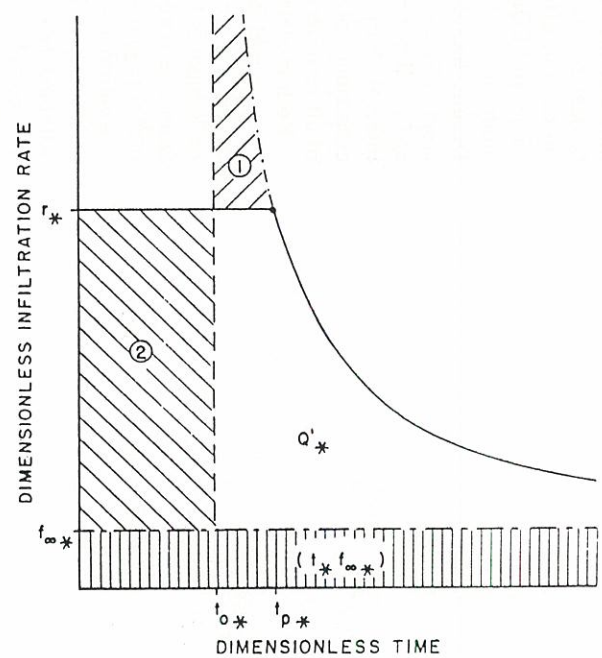

FIG. 13.—Infiltration Decay Curve as Produced by Eq. 1, Described in Terms of Soil Storage Q', Dependent Dimensionless Function

plot. In one situation, however (dry initial condition and very low intensity rainfall), the INFIL model predicted no runoff. The SEQM model predicted far less runoff than was measured, possibly because the model cannot account for variable effects of the air phase. Both methods require an initial soil moisture value. In SEQM, that value is the actual degree of saturation, and in the INFIL model it is a percentage of a conceptual soil volume filled with water (ASM). Despite the relative measure of the antecedent moisture (a resistance reading from moisture blocks), the exact initial moisture state is still somewhat uncertain and predicted outputs of the soil model implicitly incorporate a small confidence interval. Furthermore, the apparent prediction accuracy incorporates both the consistency of soil between infiltrometer plot and the test plot, and timing accuracy of all recorders.

Both models predicted rainfall excess "reasonably well." Obviously quality of measured data need improvement before better comparisons can be made. Given that prediction by these models is in some cases comparable, it should be pointed out that the four parameters of SEQM may be reasonably estimated from one (two would be better) infiltrometer test, while the empirical INFIL model requires many samples for the trial and error fits of seven parameters.

Applications in Watershed Hydrology.—Hydrologists often invoke "prediction" as a prime objective for constructing models of various hydrologic processes. Although few such models apparently ever become operational, the construction and complexity of a practical model must explicitly reflect the scale of the process to be modeled and the object of the modeling. Thus, selection among several infiltration models in describing floods on a large complex basin would probably be academic.

The question confronting a practitioner is how to select a model to serve his needs. One of the first tasks is the calibration of the model. Selection of an infiltration model should depend in part on how readily, accurately, and representatively the parameters may be determined. In this comparison, the SEQM model has significant advantages over the empirical INFIL model. It appears that the four additional parameters of the empirical INFIL model provide no detectable advantage over the SEQM model.

The representativeness of the parameters becomes a function of the soil uniformity over an area and the size of the area for which one desires to predict rainfall excess. These questions on parameter determination have not been developed, but are worthy of further investigation. It is not certain, for example, whether the description of infiltration over an area exhibiting a range of infiltration properties (or parameters) will act as an average of the contributing soils or will act in aggregate unlike any soil within the area.

Conclusions

A parametric infiltration model has been presented, SEQM, that duplicates the performance of a numerical solution describing the infiltration of water into an unsaturated porous media. The model has been used to predict runoff from small runoff plots and has been compared with a currently proposed empirical parametric model. The SEQM model, besides being physically based, appears to predict runoff adequately, and in addition, has fewer and apparently more easily determined parameters than the comparable empirical infiltration model developed by Holtan.

The model's sensitivity to rapid changes in rainfall rate is greater than the sensitivity of standard measuring equipment. Ongoing improvements in instrumentation, however, are providing data for a more thorough evaluation of the theoretically-based SEQM model. Nevertheless, the data presented herein illustrate both the practical predictive application of current soil moisture flow theory and the fact that the sophistication of the physics of watershed processes has outstripped the quality of measurement techniques currently in common use.

Appendix I.—Derivation of Eq. 7

For a case of uniform rainfall rate, we wish to show that Eq. 7 may be obtained as a solution of a nonlinear differential equation dependent on accumulated soil water. A modified form of Eq. 5 may be written

$$f'_* = \frac{dQ'_*}{dt_*} = \frac{C}{(Q'_* - Q_{o*})^n} \quad \text{(10)}$$

in which Q_{o*} = a dimensionless water storage term analogous in function to t_{o*} in Eq. 6. It may be defined as that correction necessary to make $Q'_* = Q_{o*}$ at $t_* = t_{o*}$. This is represented in Fig. 13 as area 2 less area 1. This definition recognizes that Q'_* is accumulated at rate r_* up to time t_{p*}, rather than as Eq. 10 would describe; this is not inconsistent since Eq. 10 is used only for $t_* > t_{p*}$.

Eq. 10 can be rearranged and integrated to yield

$$(Q'_* - Q_{o*})^{n+1} = (n+1)\,C\,t_* + C_1 \quad \text{(11)}$$

in which C_1 is a variable of integration, and since $Q'_* = Q_{o*}$ at $t_* = t_{o*}$, $C_1 = -(n+1)Ct_{o*}$. Thus

$$(Q'_* - Q_{o*})^{n+1} = (n+1)\,C(t_* - t_{o*}) \quad \text{(12)}$$

From Eq. 12, expression on the left side of Eq. 10 may be isolated, to obtain

$$\frac{C}{(Q'_* - Q_{o*})^n} = C^{1/n+1}\,[(t_* - t_{o*})(n+1)]^{-n/n-1} \quad \text{(13)}$$

Term by term comparison of Eq. 13 with Eq. 4 may be used to demonstrate the relations in Eq. 6.

Appendix II.—References

1. Freeze, R. A., "Role of Subsurface Flow in Generating Surface Runoff. 1. Base Flow Contribution to Channel Flow," *Water Resources Research*, Vol. 8, No. 3, June, 1972, pp. 609–623.
2. Gardner, W. R., "Development of Modern Infiltration Theory and its Application in Hydrology," *Transactions, American Society of Agricultural Engineers*, Vol. 10, No. 3, 1967, pp. 379–381.
3. Hanson, V. E., "Infiltration and Soil Water Movement During Irrigation," *Soil Science*, Vol. 79, No. 2, Feb., 1955, pp. 93–105.
4. Holtan, H. N., and Lopez, N. C., "USDAHL-70 Model of Watershed Hydrology," *Technical Bulletin No. 1435*, Agricultural Research Service, United States Dept. of Agriculture, Nov., 1971.

5. Kostiakov, A. N., "On the Dynamics of the Coefficient of Water Percolation in Soils and on the Necessity for Studying it from a Dynamic Point of View for Purposes of Amelioration," *Transactions of the Sixth Committee International Society of Soil Science*, Part A, 1932, pp. 17-21.
6. McWhorter, D. B., "Infiltration Affected by Flow of Air," *Hydrology Paper 47*, Colorado State University, Fort Collins, Colo., Apr., 1971.
7. Smith, R. E., "The Infiltration Envelope: Results From a Theoretical Infiltrometer," *Journal of Hydrology*, Vol. 17, 1972, pp. 1-21.
8. Smith, R. E., and Woolhiser, D. A., "Mathematical Simulation of Infiltrating Watersheds," *Hydrology Paper No. 47*, Colorado State University, Fort Collins, Colo.
9. Whisler, F. D., and Bouwer, H., "Comparison of Methods for Calculating Vertical Drainage and Infiltration for Soils," *Journal of Hydrology*, Vol. 10, 1970, pp. 1-19.

Appendix III.—Notation

The following symbols are used in this paper:

A = coefficient parameter in infiltration equation;
a = parameter in Holton's infiltration formula;
ASM = initial wetness of soil, percentage of available volume;
AWC = soil water drained by vegetation, percentage of total;
B = parameter in functional relation between Q_{p*} and r_*;
C = coefficient parameter in Eq. 5;
C_1 = constant of integration;
D = parameter in Eq. 9 for normalizing time $T_o = D(\theta_o - \theta_i)$;
f_o = infiltration rate, L/T;
f_c = constant rate of infiltration after prolonged wetting, L/T;
f'_* = $f_* - 1$;
f_∞ = infiltration rate at $t = \infty$, equivalent to K;
$f_{\infty*} = 1$ = dimensionless infinite infiltration rate;
G = total porosity at 0.3 bar (drained by gravity), as a percentage;
GI = growth index of crop in percent of maturity;
INFIL = acronym for subroutine in USDA Hydrograph Laboratory computer program that solves empirical infiltration model;
K = saturated conductivity, L/T;
k_r = relative permeability or conductivity;
n = exponent parameter in Eq. 5;
Q_o = reference volume, L^3;
Q_* = dimensionless infiltrated volume;
Q'_* = dimensionless accumulated soil water in excess of $(f_{\infty*}, t_*)$;
Q_{o*} = dimensionless reference volume;
Q_{p*} = Q_* at $t = t_p = t_{p*}(r_* - 1)$;
r_* = R/f_∞ = dimensionless rainfall rate;
S_a = available water storage in surface layer;
SEQM = acronym for soil-equivalent model constituted by Eqs. 7, 8, and 9;
s = variable of integration, in inches water equivalent, L;
T_o = normalizing time, defined in Eq. 3, T;
t = time, T;
t_o = reference time parameter in infiltration equation, T;
t_p = time of ponding, time at which $\psi = 0$ at surface, T;

$t_* = t/T_o$;
t_{o*} = dimensionless reference time;
t_{p*} = dimensionless time of ponding;
z = depth from soil surface L;
α = exponent parameter in infiltration equation;
β = exponent parameter, in functional relation between Q'_{p*} and r_*;
θ = water content by volume, L^3/L^3;
θ_i = initial water content;
θ_o = θ at $\psi = 0$;
ϕ = porosity, L^3/L^3; and
ψ = soil water capillary potential, L.